PHYSICAL REVIEW A **77**, 063835 (2008)

Monte Carlo simulations of pulse propagation in massive multichannel optical fiber communication systems

Yeojin Chung
Department of Mathematics, Southern Methodist University, Dallas, Texas 75275, USA

Avner Peleg
Department of Mathematics, State University of New York at Buffalo, Buffalo, New York 14260, USA

(Received 5 November 2007; revised manuscript received 13 February 2008; published 26 June 2008)

We study the combined effect of delayed Raman response and bit pattern randomness on pulse propagation in massive multichannel optical fiber communication systems. The propagation is described by a perturbed stochastic nonlinear Schrödinger equation, which takes into account changes in pulse amplitude and frequency as well as emission of continuous radiation. We perform extensive numerical simulations with the model and analyze the dynamics of the frequency moments, the bit-error rate, and the mutual distribution of amplitude and position. The results of our numerical simulations are in good agreement with theoretical predictions based on the adiabatic perturbation approach.

DOI: 10.1103/PhysRevA.77.063835 PACS number(s): 42.81.Dp, 42.65.Dr, 05.40.−a

I. INTRODUCTION

The interplay between noisy phenomena and nonlinear processes is a rich field of research that is of great interest in a variety of disciplines including solid state physics [1], turbulence [2], and optics [3]. One of the most important problems in this field concerns propagation of coherent patterns, such as solitons and solitary waves, in the presence of noise and/or disorder. An excellent example for systems where noise and nonlinear effects play an important role in the dynamics of coherent patterns is provided by fiber optics communication systems, which employ optical pulses to represent bits of information [3]. It is by now well-established that the parameters characterizing the pulses in fiber optics communication systems can exhibit non-Gaussian statistics [4–8]. Yet, since optical fiber systems are only weakly nonlinear, it was commonly believed that the statistics of optical pulses is very different from the statistics encountered in strongly nonlinear systems, such as turbulence and chaotic flow, where intermittent dynamics exists. However, a recent study of pulse propagation in optical fiber systems with multiple frequency channels in the presence of delayed Raman response obtained results that stand in sharp contrast to this common belief [9]. This study focused on the interplay between Raman-induced energy exchange in pulse collisions and randomness of pulse sequences in different frequency channels. Taking into account these two effects it was shown that the pulse parameters exhibit intermittent dynamic behavior in the sense that their normalized moments grow exponentially with propagation distance. Furthermore, it was shown that this intermittent dynamic behavior has important practical consequences, by leading to relatively large values of the bit-error-rate (BER), which is the probability for an error at the output of the fiber line.

The results of the study in Ref. [9] were based on an adiabatic perturbation procedure that neglects radiation emission effects. However, these effects can be especially important for the fiber optics system under consideration. Indeed, as we shall see below, the interplay between collision-induced energy exchange and randomness of pulse sequences can be described as an effective disorder in the linear gain/loss coefficient, and the presence of gain can lead to instability with respect to emission of continuous radiation. Therefore it is essential to obtain an improved description of pulse dynamics in the system that includes emission of continuous waves. In this paper we take this important task and derive a perturbed stochastic nonlinear Schrödinger (NLS) equation, which takes into account both changes in pulse parameters and radiation emission effects. We employ this model to analyze the dynamics of soliton parameters in comparison with the results of the simpler description of Ref. [9] and to draw conclusions on the possibility to observe intermittent dynamics in multichannel optical fiber communication systems.

In this study we consider conventional optical solitons as an example for the pulses carrying the information for the following reasons. First, the main effect of delayed Raman response on a single collision between two optical pulses, the Raman-induced energy exchange, is similar in linear transmission [10], conventional soliton transmission [11–14], and strongly dispersion-managed (DM) soliton transmission [15]. Moreover, once the interplay between this collision-induced energy exchange and bit-pattern randomness is considered, the statistics of pulse energies is similar in all three transmission formats [10,14,16–20]. Second, propagation of conventional solitons in an optical fiber is described by the NLS equation, which is an integrable model [21]. Consequently, perturbation theories employed for calculating the effects of various impairments on the soliton are more rigorous in this case than in nonintegrable cases, such as DM transmission. Third, conventional optical solitons have traditionally been considered as excellent candidates for information transmission in optical fibers [3]. Furthermore, recent advances in distributed Raman amplification techniques allow for lossless and quasilossless transmission over distances comparable with the standard interamplifier distance of fiber optics communication systems [22,23]. In such lossless systems one can expect that four-wave mixing effects would be neg-

©2008 The American Physical Society

ligible [24,25]. It should also be mentioned that state-of-the-art transmission experiments already use all-Raman distributed amplification [26,27], which is the most suitable amplification scheme for conventional solitons. The rest of the Introduction is devoted to a summary of previous research on the impact of delayed Raman response on pulse propagation in massive multichannel communication systems.

The main effect of Raman scattering on a single soliton propagating in the fiber is the self-frequency shift. This effect, which is caused by energy transfer from higher frequency components of the pulse to its lower frequency components, was first observed experimentally by Mitschke and Mollenauer [28] and explained theoretically by Gordon [29]. Following this discovery, the impact of delayed Raman response on soliton propagation in optical fibers has drawn a lot of attention [9–20,30–34]. Most significantly, the influence on two-soliton collisions was studied by numerical simulations [11,32] as well as by theoretical analysis [12,13,15]. These studies revealed that the main effect of a single two-soliton collision in the presence of delayed Raman response is an energy exchange between the colliding pulses, which leads to a change of their amplitudes (Raman-induced cross talk) [11–13,32]. The frequencies of the two solitons was also found to change as a result of the collision (Raman-induced cross-frequency shift) [11,13,32]. We emphasize that the same energy exchange takes place in collisions between strongly DM solitons [15] as well as in collisions between pulses in the linear transmission regime [10]. Furthermore, the cross-frequency shift experienced by strongly DM solitons is very similar to the one experienced by conventional solitons [15].

Raman-induced energy exchange in pulse collisions can be beneficially employed in a variety of applications, including amplification in fiber lines [35,36] and in tunable laser sources [3,37]. However, it can also have negative effects that impose severe limitations on the performance of multichannel communication systems. Indeed, it is known that the Raman-induced energy exchange in a single interchannel collision is independent of the frequency difference between the channels. Consequently, the magnitude of the induced energy shifts for a given pulse grows with the square of the number of channels, a result that is valid for linear transmission [10], conventional soliton transmission [19], and strongly DM soliton transmission [15]. Thus in a 100-channel system, for example, these effects can be larger by a factor of 2.5×10^3 compared with a two-channel system operating at the same bit rate per channel. Furthermore, since collisions with pulses from distant channels give the main contribution to energy shifts, a complete description of the dynamics must include interaction between pulses from all frequency channels. In contrast, effects of other nonlinear phenomena on pulse collisions are inversely proportional to some integer power of the frequency difference, and their cumulative influence can be adequately described by taking into account only a few neighboring channels [3,38,39].

Early studies of Raman cross talk in linear multichannel transmission systems focused on the dependence of the induced energy shifts on the total number of channels [40,41]. The combined effects of Raman cross talk and randomness of pulse sequences were also considered, and it was found that the probability distribution function (PDF) of pulse amplitudes is lognormal [10,16–18]. However, these previous studies ignored several important properties of the system, which are essential for obtaining a correct dynamical model. First, all other nonlinear processes affecting pulse propagation, such as the Raman-induced self- and cross-frequency shifts were neglected. Second, strong coupling between amplitude dynamics and the dynamics of the other pulse parameters, such as frequency, position, and phase, was not taken into account. Consequently, only the amplitude PDF was calculated, whereas a correct evaluation of system performance requires calculation of the mutual PDF of the pulse amplitude and position. Third, most studies considered only dynamic impact on performance of high frequency channels due to pulse decay, thus ignoring potential negative consequences for intermediate and low frequency channels due to large position shifts induced by relatively large amplitude values.

A more complete description of pulse propagation, which takes into account the three aforementioned factors, was developed in Refs. [9,14,19] for conventional solitons. In Ref. [19] it was shown that the PDF of the soliton amplitude is lognormal, and that the coupling between frequency dynamics and amplitude dynamics leads to an exponential growth of the first two normalized moments of the self- and cross-frequency shifts with propagation distance. A perturbed NLS equation describing the combined effects of bit pattern randomness and Raman cross talk in a *two-channel* system was derived in Ref. [14]. Numerical simulations with the latter NLS model confirmed the analytic predictions of Ref. [19]. Later on it was shown that the nth normalized moments of the self- and cross-frequency shifts increase exponentially with both propagation distance and n^2 [9]. These results, combined with similar results for the normalized moments of the amplitude [19], imply that the soliton parameters exhibit intermittent dynamics in the sense that rare but violent events associated with relatively large amplitudes and frequency shifts become important. Furthermore, it was shown that the dominant mechanism for error generation in the system at long propagation distances is related to the intermittent dynamic behavior and is due to the Raman-induced cross-frequency shift [9]. In this process the error is generated due to large values of the frequency and position shifts induced by large amplitude values. Thus it is very different from the two mechanisms for error generation that are usually considered in fiber optics transmission, which are due to: (1) position shift with almost constant amplitude and (2) amplitude decay with almost constant position shift. As mentioned above, the analysis in Ref. [9] ignored radiation emission effects, which can be important in massive multichannel transmission. In the current paper we take these effects into account and derive a perturbed stochastic NLS model for propagation in *massive* multichannel transmission systems, where the number of channels is much larger than one. We analyze the dynamics of the soliton parameters and the behavior of the bit-error-rate (BER) by extensive numerical simulations with the model, and compare our results with the analytic calculations of Ref. [9].

The material in the rest of the paper is organized as follows. In Sec. II A, we construct a perturbed stochastic NLS model describing soliton propagation in massive multichannel optical fiber transmission systems. The dynamics of the soliton amplitude and frequency and of the BER are obtained in Sec. II B by employing a standard adiabatic perturbation procedure. In Sec. III, we analyze the results of numerical simulations with the perturbed NLS model and compare them with the predictions of the adiabatic perturbation theory. Section IV is reserved for conclusions.

II. STOCHASTIC MODEL FOR PULSE PROPAGATION

A. Derivation of the model

Propagation of short pulses of light through an optical fiber in the presence of delayed Raman response is described by the following perturbed NLS equation [3]:

$$i\partial_z\psi + \partial_t^2\psi + 2|\psi|^2\psi = -\epsilon_R\psi\partial_t|\psi|^2, \tag{1}$$

where ψ is proportional to the envelope of the electric field, z is propagation distance, and t is time in the retarded reference frame. The term $-\epsilon_R\psi\partial_t|\psi|^2$ represents the first order approximation for the fiber's delayed Raman response and ϵ_R is the Raman coefficient [42]. When $\epsilon_R=0$, the single-soliton solution of Eq. (1) in a frequency channel β is given by

$$\psi_\beta(t,z) = \eta_\beta \frac{\exp(i\chi_\beta)}{\cosh(x_\beta)}, \tag{2}$$

where $x_\beta=\eta_\beta(t-y_\beta-2\beta z)$, $\chi_\beta=\alpha_\beta+\beta(t-y_\beta)+(\eta_\beta^2-\beta^2)z$, and η_β, α_β, and y_β are the soliton amplitude, phase, and position, respectively.

Consider the effects of delayed Raman response on a single collision between two solitons from different frequency channels. For simplicity, one of the two channels is chosen as the reference channel with $\beta=0$ so that the frequency difference between the two channels is β. We assume that $\epsilon_R \ll 1$ and $1/|\beta| \ll 1$, which is the typical situation in current multichannel transmission systems [43]. In addition, we assume that the two solitons are initially well-separated from each other in the temporal domain. Under these assumptions we can employ the perturbation procedure, developed in Refs. [44–46], and applied in Ref. [14] for the case of delayed Raman response. Here we only give the outline of the calculation and refer the interested reader to Ref. [14] for details. In accordance with this perturbative approach, we look for a two-pulse solution of Eq. (1) in the form

$$\psi_{two} = \psi_0 + \psi_\beta + \phi, \tag{3}$$

where ψ_0 and ψ_β are single-pulse solutions of Eq. (1) with $0<\epsilon_R\ll 1$ in channels 0 and β, respectively. The term ϕ on the right-hand side of Eq. (3) is a small correction to the single-soliton solutions, which is solely due to collision effects. By analogy with the ideal collision case we take ϕ to be of the form

$$\phi = \phi_0 + \phi_\beta + \cdots, \tag{4}$$

where ϕ_0 and ϕ_β represent collision-induced corrections in channels 0 and β, and the ellipsis represents higher order terms in other channels. Combining Eqs. (3) and (4) we see that the total pulse in the reference channel is $\psi_0^{total}=\psi_0+\phi_0$. We substitute the relations (3) and (4) together with $\psi_0(t,z)=\Psi_0(x_0)\exp(i\chi_0)$, $\phi_0(t,z)=\Phi_0(x_0)\exp(i\chi_0)$, $\psi_\beta(t,z)=\Psi_\beta(x_\beta)\exp(i\chi_\beta)$, and $\phi_\beta(t,z)=\Phi_\beta(x_\beta)\exp(i\chi_\beta)$ into Eq. (1). The resulting equation can be readily decomposed into an equation for the evolution of Φ_0 and an equation for the evolution of Φ_β. We focus attention on Φ_0 and remark that the calculation of Φ_β is very similar. The equation for Φ_0 is solved by integration with respect to z over the collision region. Carrying out this integration one obtains that the $O(\epsilon_R)$ effect of the collision on the reference channel soliton is given by

$$\Delta\Phi_{01}^{(1)} = \eta_\beta\,\mathrm{sgn}(\beta)\epsilon_R\Psi_0(x_0), \tag{5}$$

where the first subscript in $\Delta\Phi_{01}^{(1)}$ stands for the channel, the second subscript indicates the combined order with respect to both ϵ_R and $1/\beta$, and the superscript represents the order in ϵ_R. This $O(\epsilon_R)$ effect corresponds to an amplitude change [11–14]

$$\Delta\eta_0 = 2\eta_0\eta_\beta\,\mathrm{sgn}(\beta)\epsilon_R, \tag{6}$$

which is accompanied by emission of continuous radiation. In a similar manner, one finds that the effect of the collision in order ϵ_R/β is [14]

$$\Delta\Phi_{02}^{(1)} = \frac{4i\eta_\beta\epsilon_R}{|\beta|}\partial_t\Psi_0(x_0). \tag{7}$$

$\Delta\Phi_{02}^{(1)}$ corresponds to a collision-induced frequency shift:

$$\Delta\beta_0 = -(8\eta_0^2\eta_\beta\epsilon_R)/(3|\beta|), \tag{8}$$

which is also accompanied by emission of continuous radiation.

Let us describe propagation of a reference channel soliton under many collisions with solitons from all other frequency channels in a system with $2N+1$ channels, where $N \gg 1$. We employ a mean-field approximation [14], in which we assume that the amplitudes of the solitons in the other channels are constant. The random character of soliton sequences in different channels is taken into account by defining discrete random variables ζ_{ij}, which describe the occupation state of the jth time slot in the ith channel: $\zeta_{ij}=1$ with probability s if the slot is occupied, and 0 with probability $1-s$ otherwise. It follows that the nth moment of ζ_{ij} satisfies $\langle\zeta_{ij}^n\rangle=s$. We also assume that the occupation states of different time slots are uncorrelated: $\langle\zeta_{ij}\zeta_{i'j'}\rangle=s^2$ if $i\neq i'$ and $j\neq j'$. We denote by $\Delta\beta$ the frequency difference between neighboring channels and by T the time slot width. Therefore the distance traveled by the reference channel soliton while passing two successive time slots in the nearby channels is $\Delta z_c^{(1)}=T/(2\Delta\beta)$. The $O(\epsilon_R)$ effect of the collisions is taken into account by introducing a new perturbation term S_1 into Eq. (1). The term S_1 is obtained by summing Eq. (5) over all collisions occurring in the interval $\Delta z_c^{(1)}$, and dividing the result by $\Delta z_c^{(1)}$,

$$S_1 \equiv i\epsilon_R\Psi_0 e^{i\chi_0}\sum_{i\neq 0}\mathrm{sgn}(\beta_i)\sum_{j=(k-1)i+1}^{ki}\frac{\zeta_{ij}}{\Delta z_c^{(1)}}, \tag{9}$$

where $k-1$ and k are the indexes of the two successive time slots in the $i=-1$ channel, and the outside sum is from $-N$ to N. We decompose the disorder ζ_{ij} into an average part and a fluctuating part: $\zeta_{ij}=s+\tilde{\zeta}_{ij}$, where $\langle\tilde{\zeta}_{ij}\rangle=0$, $\langle\tilde{\zeta}_{ij}\tilde{\zeta}_{i'j'}\rangle=s(1-s)\delta_{ii'}\delta_{jj'}$, and $\delta_{ii'}$ is the Kronecker delta function. Substituting $\zeta_{ij}=s+\tilde{\zeta}_{ij}$ into Eq. (9) we obtain

$$S_1=\frac{2is\epsilon_R\Delta\beta\psi_0}{T}\sum_{i\neq 0}\mathrm{sgn}(\beta_i)|i|+i\epsilon_R\xi(z)\psi_0, \tag{10}$$

where the continuous disorder field $\xi(z)$ is

$$\xi(z)=\frac{1}{\Delta z_c^{(1)}}\sum_{i\neq 0}\mathrm{sgn}(\beta_i)\sum_{j=(k-1)i+1}^{ki}\tilde{\zeta}_{ij}. \tag{11}$$

Using Eq. (11) and the properties of ζ_{ij} one can show that $\langle\xi(z)\rangle=0$ and $\langle\xi(z)\xi(z')\rangle=D_N\delta(z-z')$, where $D_N=N(N+1)D_2$, $D_2=2\Delta\beta s(1-s)T^{-1}$, and $\delta(z)$ is the Dirac delta function. Notice that the first term on the right-hand side of Eq. (10) is zero due to symmetry. Even if this term is not zero, it can be compensated by appropriately adjusting the gain of the amplifiers. Therefore the $O(\epsilon_R)$ effect of the collisions is described by

$$S_1=i\epsilon_R\xi(z)\psi_0. \tag{12}$$

The $O(\epsilon_R/\beta)$ effect of the collisions is calculated in a similar manner. We first sum Eq. (7) over all collisions occurring within the interval $\Delta z_c^{(1)}$:

$$\tilde{S}_2\equiv -c_1\partial_t\Psi_0-4\epsilon_R\partial_t\Psi_0\sum_{i\neq 0}\frac{1}{|\beta_i|}\sum_{j=(k-1)i+1}^{ki}\frac{\tilde{\zeta}_{ij}}{\Delta z_c^{(1)}}, \tag{13}$$

where $c_1=(16N\epsilon_R s)/T$. The second term on the right-hand side of Eq. (13) can be estimated as $-8[D_2H_N/(T\Delta\beta)]^{1/2}\epsilon_R\partial_t\Psi_0$, where $H_N=\Sigma_{j=1}^{N}1/j$. Consequently, for a typical multichannel system the coefficient in front of $\epsilon_R\partial_t\Psi_0$ in this term is of order 1 or smaller, whereas for the first term this coefficient is of order N. We therefore neglect the second term on the right-hand side of Eq. (13), and set $\tilde{S}_2=-c_1\partial_t\Psi_0$. Using the fact that for a weakly perturbed soliton $e^{i\chi_0}\partial_t\Psi_0=\partial_t\psi_0-i\beta_0\psi_0$ we arrive at

$$S_2\equiv e^{i\chi_0}\tilde{S}_2=-c_1\partial_t\psi_0+ic_1\beta_0\psi_0, \tag{14}$$

where β_0 is the frequency of the perturbed reference channel soliton. Substituting S_1 and S_2 into Eq. (1) and replacing ψ_0 with ψ we obtain

$$\begin{aligned}i\partial_z\psi+\partial_t^2\psi+2|\psi|^2\psi={}&-\epsilon_R\psi\partial_t|\psi|^2+i\epsilon_R\xi(z)\psi-c_1\partial_t\psi\\&+ic_1\beta_0(z)\psi,\end{aligned} \tag{15}$$

which is the stochastic model describing propagation of the reference channel soliton in the fiber under many collisions.

We remark that in Ref. [14] the second term on the right-hand side of Eq. (13) was taken into account, whereas the first term was neglected. Therefore the perturbed NLS model derived in Ref. [14] is unsuitable for describing pulse dynamics in massive multichannel transmission. We also note that in deriving Eq. (15) we neglect the position shift induced by the influence of Kerr nonlinearity on the collisions. This approximation is justified in the Appendix, where we show that the magnitude of the position shift induced by the terms on the right-hand side of Eq. (15) is much larger compared with the position shift due to Kerr nonlinearity for intermediate and large propagation distances.

B. Statistics of soliton parameters and BER calculation

The evolution of the parameters of the reference channel soliton with propagation distance can be obtained by employing the standard adiabatic perturbation theory [47,48]. Employing this perturbation procedure we obtain the following equations for the soliton amplitude and frequency:

$$\frac{d\eta_0}{dz}=2\epsilon_R\xi(z)\eta_0(z) \tag{16}$$

and

$$\frac{d\beta_0}{dz}=-\frac{8}{15}\epsilon_R\eta_0^4(z)-\frac{2}{3}c_1\eta_0^2(z). \tag{17}$$

Notice that the right-hand side of Eq. (16) is contributed solely by the second term on the right-hand side of Eq. (15), i.e., the term describing the Raman cross talk effects. The first and second terms on the right-hand side of Eq. (17) describe the Raman-induced self- and cross-frequency shifts, and are contributed by the first and third terms on the right-hand side of Eq. (15), respectively.

Integrating Eq. (16) over z we obtain

$$\eta_0(z)=\eta_0(0)\exp[2\epsilon_R x(z)], \tag{18}$$

where $x(z)=\int_0^z dz'\,\xi(z')$ and $\eta_0(0)$ is the initial amplitude. According to the central limit theorem, the PDF of $x(z)$ approaches a Gaussian PDF with $\langle x(z)\rangle=0$ and $\langle x^2(z)\rangle=D_N z$. As a result, the PDF of the soliton amplitude approaches a lognormal PDF:

$$F(\eta_0)=(8\pi D_N\epsilon_R^2 z)^{-1/2}\eta_0^{-1}\exp\left\{-\frac{\ln^2[\eta_0/\eta_0(0)]}{8D_N\epsilon_R^2 z}\right\}. \tag{19}$$

The lognormal distribution is very different from the Gaussian distribution, and this difference is significant already in the main body of the distribution [14]. Moreover, the normalized moments of the lognormal PDF grow exponentially with propagation distance, from which it follows that the soliton amplitude exhibits intermittent dynamic behavior [9].

The dynamic evolution of the soliton frequency is given by

$$\beta_0(z)=\beta_0^{(s)}(z)+\beta_0^{(c)}(z), \tag{20}$$

where

$$\beta_0^{(s)}(z)=-\frac{8}{15}\epsilon_R\int_0^z dz'\,\eta_0^4(z') \tag{21}$$

is the self-frequency shift and

$$\beta_0^{(c)}(z)=-\frac{32N\epsilon_R s}{3T}\int_0^z dz'\,\eta_0^2(z') \tag{22}$$

is the cross-frequency shift. The nth moments of $\beta_0^{(s)}$ and $\beta_0^{(c)}$ can be calculated from [9]

$$\langle\beta_0^{(s)n}(z)\rangle = \left[-\frac{8}{15}\epsilon_R\eta_0^4(0)\right]^n n\,!\prod_{m=1}^{n}\int_0^{z_{m-1}} dz_m \times\exp[32D_N\epsilon_R^2(2m-1)z_m] \tag{23}$$

and

$$\langle\beta_0^{(c)n}(z)\rangle = \left[-\frac{2}{3}c_1\eta_0^2(0)\right]^n n\,!\prod_{m=1}^{n}\int_0^{z_{m-1}} dz_m \times\exp[8D_N\epsilon_R^2(2m-1)z_m], \tag{24}$$

where $z_0=z$. By carrying out the integration in Eqs. (23) and (24) one can show that $\langle\beta_0^{(s)n}(z)\rangle$ and $\langle\beta_0^{(c)n}(z)\rangle$ are given by sums over exponential terms of the form $K_m\exp[a^{(s,c)}m^2D_N\epsilon_R^2z]$, where $a^{(s)}=32$, $a^{(c)}=8$, $0\leq m\leq n$, and the K_m are constants. Furthermore, the leading contributions to the normalized moments $\langle\beta_0^{(s)n}(z)\rangle/\langle\beta_0^{(s)}(z)\rangle^n$ and $\langle\beta_0^{(c)n}(z)\rangle/\langle\beta_0^{(c)}(z)\rangle^n$ are exponentially increasing with both z and n^2. As we shall see in the next section, the normalized fourth moments of $\beta_0^{(s)}$, $\beta_0^{(c)}$, and β_0 increase much faster with increasing propagation distance compared with the normalized second and third moments, which is a consequence of the intermittent nature of the dynamics.

In order to evaluate the system's BER we need to consider the main dynamical mechanisms leading to error generation. One mechanism, which has been widely studied in relation with Raman cross talk [10,16–18,40,41], is due to pulse decay induced by loss of energy in collisions. This mechanism is associated with the small-η tail of the amplitude PDF. Another mechanism, which has only recently been studied in relation with Raman cross talk, is due to the interplay between frequency (and position) dynamics and amplitude dynamics [9]. In this case, the error is generated due to large values of the position shift, which are associated with large frequency shifts, and induced by relatively large values of the soliton amplitude. Notice that the lognormal statistics of the soliton amplitude leads to further enhancement of the BER contribution from the latter mechanism, since the large-η tail of the lognormal PDF lies above the corresponding tail of the Gaussian PDF. We are therefore interested in the soliton position shift, which is given by

$$y_0(z) = y_0^{(s)}(z) + y_0^{(c)}(z), \tag{25}$$

where

$$y_0^{(s)}(z) = -\frac{16\epsilon_R}{15}\int_0^z dz'\int_0^{z'} dz''\,\eta_0^4(z'') \tag{26}$$

and

$$y_0^{(c)}(z) = -\frac{64N\epsilon_R s}{3T}\int_0^z dz'\int_0^{z'} dz''\,\eta_0^2(z'') \tag{27}$$

are the contributions from the self- and cross-frequency shifts, respectively. The position shift with a fixed amplitude $\eta_0(z)=\eta_0(0)=1$ is $\tilde{y}_0(z)=\tilde{y}_0^{(s)}(z)+\tilde{y}_0^{(c)}(z)$, where $\tilde{y}_0^{(s)}(z)=-(8\epsilon_Rz^2)/15$ and $\tilde{y}_0^{(c)}(z)=-(32N\epsilon_Rsz^2)/(3T)$. The relative position shift is $\Delta y_0(z)=\Delta y_0^{(s)}(z)+\Delta y_0^{(c)}(z)$, where $\Delta y_0^{(s)}(z)=y_0^{(s)}(z)-\tilde{y}_0^{(s)}(z)$ and $\Delta y_0^{(c)}(z)=y_0^{(c)}(z)-\tilde{y}_0^{(c)}(z)$. We assume that $\tilde{y}_0$ can be compensated by employing filters. Therefore the energy measured by the detector at a distance z is

$$I(\eta_0,\Delta y_0) = \eta_0^2\int_{-T/2}^{T/2} dt\,\cosh^{-2}[\eta_0(t-\Delta y_0)]. \tag{28}$$

An occupied time slot is considered to be in error if $I(\eta_0,\Delta y_0)\leq I(z=0)/2\simeq 1$. We estimate the BER by numerically integrating Eqs. (26) and (27) coupled to Eq. (18) for different realizations of the disorder $\xi(z)$ and calculating the fraction of errored occupied time slots. The z dependence of the BER obtained by this calculation is described in Sec. III.

III. NUMERICAL SIMULATIONS

In the previous section we calculated the statistics of the soliton parameters and the BER by employing the adiabatic perturbation theory and neglecting effects associated with emission of continuous radiation. We note that the latter effects can be particularly important for the system described by Eq. (15). Indeed, the second term on the right-hand side of this equation has the form of disorder in the linear gain/loss coefficient. Such a term can lead to instability with respect to emission of continuous radiation, which is of second order in ϵ_R. It is therefore important to compare the results obtained in the previous section by the reduced adiabatic method with results of numerical simulations with the more complete model, described by Eq. (15).

Notice that the fourth term on the right-hand side of Eq. (15) includes β_0. Since both β_0 and c_1 are of order ϵ_R this term is of order ϵ_R^2, whereas the other perturbation terms in the equation are of order ϵ_R. Moreover, since β_0 is a z-dependent random variable it is computationally complicated to solve Eq. (15) in its exact form. To overcome this problem, we replace β_0 in Eq. (15) with its value for the case where the amplitude is fixed and equal to 1: $\tilde{\beta}_0(z)=-(32N\epsilon_Rsz)/(3T)-(8\epsilon_Rz)/15$. Thus the perturbed NLS which we solve numerically is

$$i\partial_z\psi+\partial_t^2\psi+2|\psi|^2\psi = -\epsilon_R\psi\partial_t|\psi|^2 + i\epsilon_R\xi(z)\psi - c_1\partial_t\psi + ic_1\tilde{\beta}_0(z)\psi. \tag{29}$$

The initial condition is taken in the form of an ideal soliton: $\psi(t,z=0)=\cosh^{-1}(t)$, with $\eta_0(0)=1$, $\beta_0(0)=0$, $y_0(0)=0$, and $\alpha_0(0)=0$.

We perform Monte Carlo simulations with Eq. (29) with about 5×10^4 disorder realizations. The equation is integrated by employing the split-step method with periodic boundary conditions. Numerical errors resulting from radiation emission and the use of periodic boundary conditions are overcome by applying artificial damping at the vicinity of the boundaries of the computational domain. The size of the domain is taken to be $-100\leq t\leq 100$ so that the absorbing layers do not affect the dynamics of the soliton pulses. The t step and z step are taken as $\Delta t=0.048$ and $\Delta z=0.001$, respectively.

We focus attention on a transmission system with 101 channels operating at 10 Gbits/s per channel. It should be emphasized that state-of-the-art experiments with dispersion-managed solitons demonstrated multichannel transmission with 109 channels at 10 Gbits/s per channel over a distance of 2×10^4 km [26]. Several other experiments achieved total bit-rate capacities exceeding 1 Tbits/s for shorter propagation distances [27,49,50]. We use the following set of parameters, which is similar to the one used in multichannel transmission experiments with conventional solitons [43]. Assuming that $T=5$, $\Delta\beta=10$, $s=1/2$, and $\eta_i(0)=1$ for all channels, the pulse width is 20 ps, $\epsilon_R=3\times 10^{-4}$, the channel spacing is 75 GHz, and $D_2=1$. Taking $\beta_2=-1$ ps^2/km, the soliton peak power is $P_0=1.25$ mW. For these values the width of the lognormal PDF in Eq. (19), which represents the strength of disorder effects, is $8D_N\epsilon_R^2 z=1.8\times 10^{-3}z$ for the reference channel. For $z=25$, corresponding to transmission over 2×10^4 km, $8D_N\epsilon_R^2 z=0.046$.

The z dependences of the $n=2,3,4$ normalized moments of $\beta_0^{(s)}$, $\beta_0^{(c)}$, and β_0 as obtained by numerical solution of the perturbed NLS are shown in Fig. 1 together with the results of the adiabatic perturbation theory. The numerical simulation results for $\beta_0^{(s)}$ and $\beta_0^{(c)}$ were obtained by solving the reduced models

$$i\partial_z\psi+\partial_t^2\psi+2|\psi|^2\psi=-\epsilon_R\psi\partial_t|\psi|^2+i\epsilon_R\xi(z)\psi \tag{30}$$

and

$$i\partial_z\psi+\partial_t^2\psi+2|\psi|^2\psi=i\epsilon_R\xi(z)\psi-c_1\partial_t\psi+ic_1\tilde{\beta}_0(z)\psi \tag{31}$$

with $\tilde{\beta}_0(z)=-(32N\epsilon_R sz)/(3T)$, respectively. The results obtained by numerical solution of the perturbed NLS equation are in good agreement with those obtained by the adiabatic perturbation theory. Moreover, one can see that the fourth moments of $\beta_0^{(s)}$, $\beta_0^{(c)}$, and β_0 increase much faster with increasing z compared with the second and third moments, in accordance with the intermittent nature of the dynamics. In addition, the normalized moments of $\beta_0^{(s)}$ grow faster than those of $\beta_0^{(c)}$. This can be explained by noting that the rate of change of $\beta_0^{(s)}$ is proportional to η_0^4, whereas $d\beta_0^{(c)}/dz$ is proportional to η_0^2. Notice, however, that the values of the normalized moments of the total frequency shift β_0 are very close to those of $\beta_0^{(c)}$. This is due to the fact that for the system described above $\beta_0^{(c)}$ is typically much larger than $\beta_0^{(s)}$.

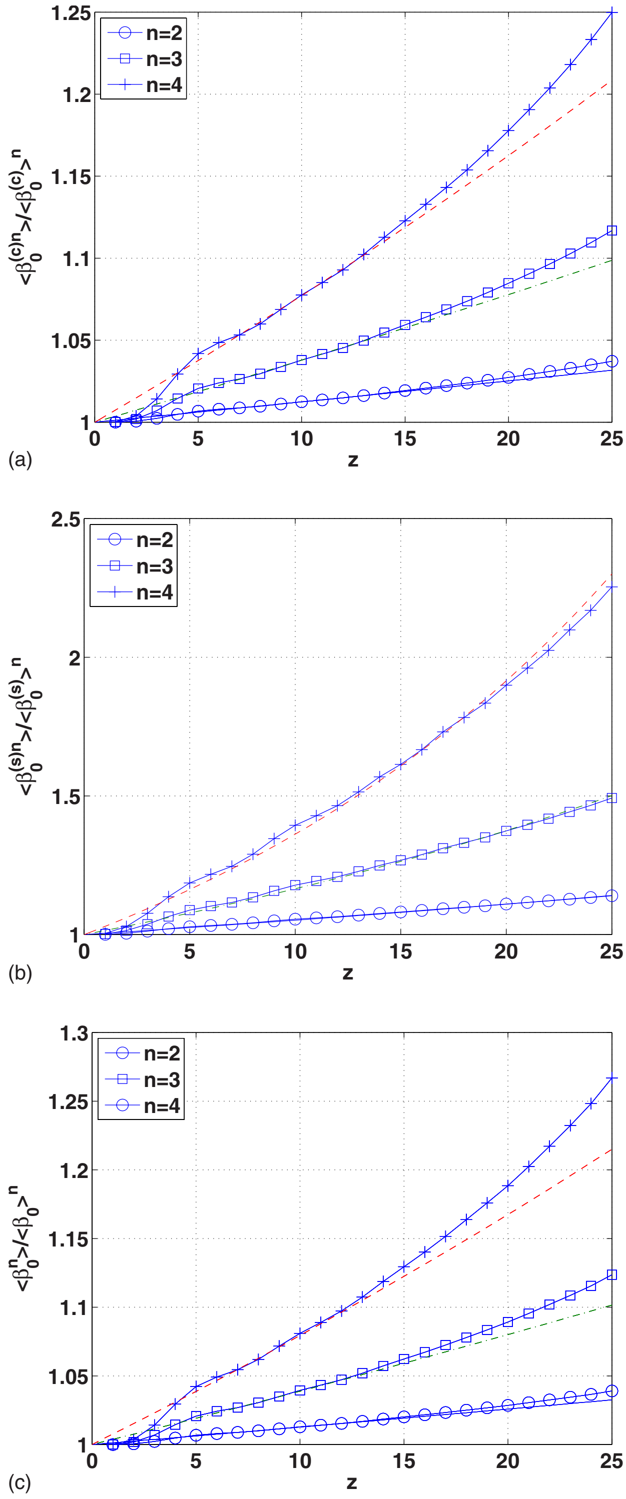

FIG. 1. (Color online) Normalized moments of the reference channel soliton's cross-frequency shift (a), self-frequency shift (b), and total frequency shift (c) vs propagation distance z for a multichannel system with 101 channels at 10 Gbits/s per channel. The solid, dashed-dotted, and dashed lines correspond to the $n=2,3,4$ normalized moments obtained by the adiabatic perturbation method, using Eqs. (22) and (24) in (a), Eqs. (21) and (23) in (b), and Eqs. (20)–(22) in (c). The circles, squares, and crosses represent the $n=2,3,4$ normalized moments obtained by numerical integration of Eq. (31) in (a), Eq. (30) in (b), and Eq. (29) in (c).

The BER of the reference channel is calculated by the procedure described in Sec. II B. That is, we calculate the measured intensity using Eq. (28), and declare an occupied time slot to be in error if $I(\eta_0,\Delta y_0)\le I(z=0)/2\simeq 1$. The z dependence of the BER obtained by numerical integration of Eq. (29) is shown in Fig. 2 together with the result obtained by employing the adiabatic perturbation procedure. The agreement between the perturbed NLS simulations and the corresponding adiabatic theory calculations is good. Furthermore, it is seen that the BER attains relatively large values, which range from about 3×10^{-5} for $z=16$ ($X=1.28\times 10^4$ km) to about 10^{-1} at $z=25.0$ ($X=2\times 10^4$ km). We remark that the BER values obtained by integrating Eq. (31), which takes into account only $y_0^{(c)}$, are very close to the ones obtained by solving Eq. (29), which takes into account both $y_0^{(s)}$ and $y_0^{(c)}$. In fact, since the difference between the two

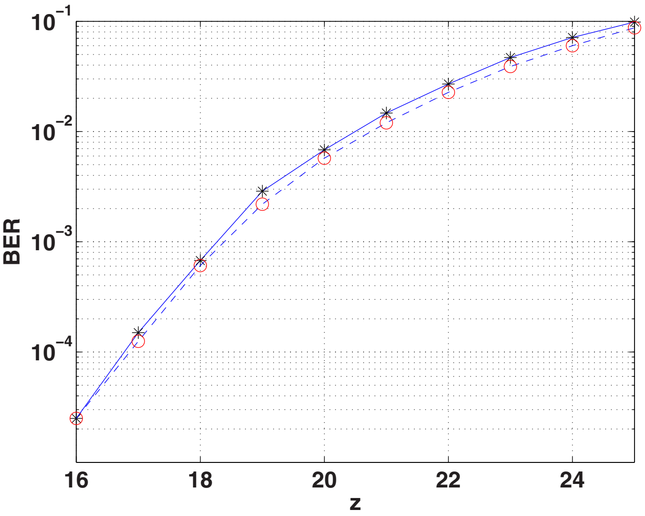

FIG. 2. (Color online) The z dependence of the BER for the reference channel in a 101-channel transmission system operating at 10 Gbits/s per channel. The circles represent the adiabatic perturbation prediction obtained by using Eqs. (18), (26), and (27), while the stars correspond to the result of numerically integrating Eq. (29).

BER curves is indistinguishable on the scale of Fig. 2, we choose to omit the result obtained with Eq. (31). The fact that the two models [Eqs. (29) and (31)] give such close BER values is explained by noting that the cross-frequency shift is typically much larger than the self-frequency shift for the multichannel system considered here.

As explained in Sec. II and in Ref. [9], the two main mechanisms for error generation in the multichannel system are (1) pulse decay and (2) large position shifts. While the first mechanism is associated with small pulse amplitudes, the second one is predominantly due to large amplitudes. Hence in order to better understand the roles of these two error-generating mechanisms one has to study the mutual PDF $G(\eta_0,\Delta y_0)$. Figure 3 shows $G(\eta_0,\Delta y_0)$ for the reference channel soliton at the final propagation distance $z=25$. The result obtained by numerical solution of Eq. (29) [Fig. 3(a)] is in good agreement with the prediction of the adiabatic perturbation theory [Fig. 3(b)]. Moreover, the mutual distribution function is strongly asymmetric about the $\Delta y_0=0$ and $\eta_0=1$ axes. This asymmetry is a direct consequence of the strong coupling between position dynamics and amplitude dynamics, as can be seen from Eqs. (26) and (27). We emphasize that this behavior is very different from the one observed for soliton propagation in single-channel systems in the presence of amplifier noise, where the mutual PDF is approximately symmetric with respect to both $\Delta y_0=0$ and $\eta_0=1$ [6,8]. We also note that the mutual PDF shown in Fig. 3 is skewed toward larger η_0 values, which can be explained by the skewed character of the lognormal distribution $F(\eta_0)$.

IV. CONCLUSIONS

We investigated propagation of optical pulses in *massive* multichannel optical fiber communication systems, focusing on the interplay between delayed Raman response and bit pattern randomness. We derived a mean-field description of the propagation, which is given by a perturbed stochastic NLS equation that takes into account changes in pulse energy and momentum. This perturbed NLS model includes the effects of emission of continuous radiation, which were neglected in the simpler adiabatic perturbative approach used in Ref. [9]. The inclusion of radiation emission effects is especially important for massive multichannel setups, since the interplay between Raman cross talk and bit pattern randomness can be described as disorder in the linear gain coefficient, and such disorder leads to an instability of the radiative modes. Our numerical simulations with the stochastic NLS model show that the normalized moments of the soliton frequency shift grow exponentially with propagation distance. Furthermore, the dynamics leads to relatively high values of the BER at intermediate and large propagation distances and to an asymmetric form of the mutual PDF of amplitude and position. The main contribution to the soliton's position shift and BER is due to the s-dependent part of the Raman-induced cross-frequency shift, an effect that was neglected in a previous treatment of *two-channel* systems [14]. The numerical simulations results are compared with predictions of the reduced adiabatic perturbation theory. This comparison is a crucial step toward achieving a full understanding of the problem, since the soliton's position and amplitude shifts at intermediate and long propagation distances are relatively large, and there is no guarantee that a reduced perturbative description would hold in this case. Based on the good agreement between simulations and perturbation theory we conclude that the interplay between Raman scattering and bit pattern randomness plays a very important role in massive multichannel transmission systems.

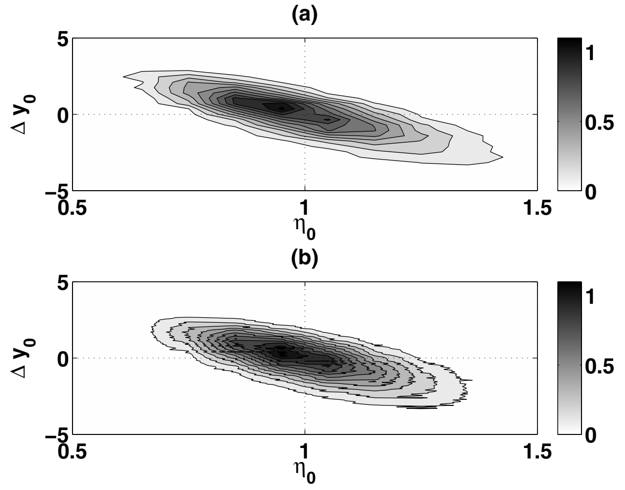

FIG. 3. Mutual PDF $G(\eta_0,\Delta y_0)$ for the reference channel soliton at $z=25$ as obtained by numerical integration of Eq. (29) (a), and as predicted by the adiabatic perturbation method (b).

The exponential growth of the normalized moments of soliton parameters is indicative of intermittent dynamics in the following sense: for certain realizations of pulse sequences (in the other frequency channels) the reference channel soliton can experience relatively large changes in its amplitude, which lead to relatively large position shifts and BER values. This dynamic behavior is quite surprising, since intermittency is usually associated with strongly nonlinear systems such as turbulence and chaotic flow [2], whereas optical fiber systems are only weakly nonlinear. In a recent paper [51], one of the authors suggested that this unexpected similarity might not be coincidental, but rather a consequence of the similarity between the dynamic behavior of the soliton amplitude in the fiber optics system and the behavior of the local average of energy dissipation in turbulent flow.

Note that the dynamic behavior described in the current paper is not limited to conventional optical solitons. Indeed, it is known that the effects of delayed Raman response on a single collision between two strongly DM solitons are very similar to the effects in the conventional soliton case [15]. Therefore we expect that similar results would hold for DM multichannel transmission systems as well. A different type of nonlinearity that can lead to similar dynamics is due to nonlinear loss/gain. In this case pulse propagation is described by a perturbed NLS equation, in which the $-\epsilon_R \psi \partial_t |\psi|^2$ term is replaced by $\mp \epsilon_c |\psi|^2 \psi$, where ϵ_c is the cubic nonlinear loss/gain coefficient. It can be shown that the main effect of a fast collision in the presence of nonlinear loss/gain is a change in the soliton amplitude, which is given by an equation of the form (6) with $\mathrm{sgn}(\beta)\epsilon_R$ replaced by $\mp 2\epsilon_c/|\beta|$. If additional perturbations that affect the soliton frequency and position exist, the dynamics of the frequency or position will usually be coupled to the amplitude dynamics in a manner similar to the one described in Sec. II. Consequently, our results should also be applicable for propagation of NLS solitons in systems with nonlinear loss or gain.

We conclude by remarking that the stochastic NLS model developed in the current paper is still an approximate description of the actual dynamics. Thus it would be interesting to compare the results of numerical simulations with this stochastic model with full-scale numerical simulations with Eq. (1) and random initial conditions in all channels.

APPENDIX: COMPARISON OF POSITION SHIFTS INDUCED BY DELAYED RAMAN RESPONSE AND KERR NONLINEARITY

In this Appendix we compare the magnitudes of the position shift induced by the Raman cross-frequency shift and the position shift caused due to the influence of Kerr nonlinearity on the collisions. The latter effect is considered to be dominant in few-channel soliton-based transmission systems [43]. The comparison is done by calculating the average of the second moment for these two positions shifts.

1. Position shift due to Kerr nonlinearity

The position shift experienced by a reference-channel soliton in a single collision with a β-channel soliton in the presence of Kerr nonlinearity is given by (see, e.g., [14,43])

$$\Delta y_0^{(K)} = \frac{4\,\mathrm{sgn}(\beta)\,\eta_\beta}{\beta^2}. \tag{A1}$$

The dynamic equation for the position of the reference channel soliton is obtained by summing over all collisions occurring within the interval $\Delta z_c^{(1)}$, dividing by $\Delta z_c^{(1)}$, and going to the continuum limit. This calculation yields

$$\frac{dy_0^{(K)}}{dz} = \frac{8s}{T\Delta\beta}\sum_{i\neq 0}\frac{\mathrm{sgn}(\beta_i)}{|i|} + 4\Theta(z), \tag{A2}$$

where

$$\Theta(z) = \frac{1}{\Delta z_c^{(1)}}\sum_{i\neq 0}\frac{\mathrm{sgn}(\beta_i)}{\beta_i^2}\sum_{j=(k-1)i+1}^{ki}\tilde{\zeta}_{ij}. \tag{A3}$$

From Eq. (A3) it follows that $\langle\Theta(z)\rangle=0$ and $\langle\Theta(z)\Theta(z')\rangle = D_\Theta \delta(z-z')$, where

$$D_\Theta = \frac{4s(1-s)}{T\Delta\beta^3}\sum_{i=1}^{N}\frac{1}{i^3}. \tag{A4}$$

Notice that the first term on the right-hand side of Eq. (A2) is zero due to symmetry. Even when this term is nonzero, it is the same for all pulses within the same channel, and thus can be compensated for. Therefore the stochastic effects of collision-induced position shifts due to Kerr nonlinearity are described by

$$y_0^{(K)}(z) = 4\int_0^z dz'\,\Theta(z'). \tag{A5}$$

Employing Eq. (A3) and the central limit theorem we obtain that the PDF of $y_0^{(K)}(z)$ approaches a Gaussian distribution with $\langle y_0^{(K)}(z)\rangle=0$, and

$$\langle y_0^{(K)2}(z)\rangle = 16 D_\Theta z. \tag{A6}$$

Notice that $\langle y_0^{(K)2}(z)\rangle$ grows only linearly with increasing z and decreases like $\Delta\beta^{-3}$ with increasing $\Delta\beta$.

2. Position shift due to the Raman cross-frequency shift

We now estimate the magnitude of the position shift induced by the Raman cross-frequency shift. From Eq. (27) and the definition of $\Delta y_0^{(c)}(z)$ it follows that

$$\langle \Delta y_0^{(c)2}(z)\rangle = \langle y_0^{(c)2}(z)\rangle - 2\tilde{y}_0^{(c)}(z)\langle y_0^{(c)}(z)\rangle + \tilde{y}_0^{(c)2}(z). \tag{A7}$$

The term $\langle y_0^{(c)2}(z)\rangle$ is given by

$$\langle y_0^{(c)2}(z)\rangle = \left(\frac{64N\epsilon_R s}{3T}\right)^2 \int_0^z dz_1 \int_0^z dz_3 \int_0^{z_1} dz_2 \int_0^{z_3} dz_4 \times \langle \eta_0^2(z_2)\,\eta_0^2(z_4)\rangle. \tag{A8}$$

Since the expression on the right-hand side of Eq. (A8) is invariant under the exchange of z_1 with z_3 and z_2 with z_4 we obtain

$$\langle y_0^{(c)2}(z)\rangle = 2\left(\frac{64N\epsilon_R s}{3T}\right)^2 \int_0^z dz_1 \int_0^{z_1} dz_3 \int_0^{z_1} dz_2 \int_0^{z_3} dz_4 \times \langle \eta_0^2(z_2)\,\eta_0^2(z_4)\rangle. \tag{A9}$$

The two inner integrals can be decomposed in the following manner:

$$\int_0^{z_1} dz_2 \int_0^{z_3} dz_4 \langle \eta_0^2(z_2)\,\eta_0^2(z_4)\rangle = 2\int_0^{z_3} dz_2 \int_0^{z_2} dz_4 \langle \eta_0^2(z_2)\,\eta_0^2(z_4)\rangle + \int_{z_3}^{z_1} dz_2 \int_0^{z_3} dz_4 \langle \eta_0^2(z_2)\,\eta_0^2(z_4)\rangle. \qquad \text{(A10)}$$

Notice that in both double integrals in Eq. (A10) $z_2 > z_4$ in the inner integral. Therefore we can use

$$\langle \eta_0^2(z_2)\,\eta_0^2(z_4)\rangle = \eta_0^4(0)\exp[8D_N\epsilon_R^2(z_2+3z_4)]. \qquad \text{(A11)}$$

Substituting Eqs. (A9)–(A11) into Eq. (A8) and performing integration yields

$$\langle y_0^{(c)2}(z)\rangle = \left[\frac{Ns}{36TD_N^2\epsilon_R^3}\right]^2 [5\exp(32D_N\epsilon_R^2 z) - 32\exp(8D_N\epsilon_R^2 z) \times (1+24D_N\epsilon_R^2 z) + 9(3+96D_N\epsilon_R^2 z + 512D_N^2\epsilon_R^4 z^2)], \qquad \text{(A12)}$$

where $\eta_0(0)=1$ is used. Notice that the first term inside the square brackets on the right-hand side of Eq. (A12) grows exponentially with both N^2 and z. The second and third terms on the right-hand side of Eq. (A7) are given by

$$2\tilde{y}_0^{(c)}(z)\langle y_0^{(c)}(z)\rangle = \left[\frac{8Ns}{3TD_N\epsilon_R}\right]^2 z^2[\exp(8D_N\epsilon_R^2 z) - 8D_N\epsilon_R^2 z - 1] \qquad \text{(A13)}$$

and

$$\tilde{y}_0^{(c)2}(z) = \left[\frac{32N\epsilon_R s}{3T}\right]^2 z^4. \qquad \text{(A14)}$$

Using Eqs. (A7) and (A12)–(A14) we calculate the z dependence of $\langle \Delta y_0^{(c)2}\rangle$ and compare the result with the z dependence of $\langle y_0^{(K)2}\rangle$. This comparison is performed for the following three sets of parameters: (A) $\Delta\beta=10$ and $N=50$, (B) $\Delta\beta=7$ and $N=50$, and (C) $\Delta\beta=7$ and $N=64$, where the other parameters are the same as the ones considered in Sec. III. Setup A corresponds to the 101-channel system discussed in Sec. III, setup B to a 101-channel system with 50 GHz channel spacing, and setup C to a 129-channel system with 50 GHz channel spacing. The comparison is shown in Fig. 4. It is seen that $\langle \Delta y_0^{(c)2}\rangle$ exceeds $\langle y_0^{(K)2}\rangle$ for intermediate propagation distances for all three setups. Moreover, for large propagation distances $\langle y_0^{(K)2}\rangle$ is smaller than $\langle \Delta y_0^{(c)2}\rangle$ by more than an order of magnitude. In addition, while $\langle \Delta y_0^{(c)2}\rangle$ increases significantly with an increasing number of channels, the N dependence of $\langle \Delta y_0^{(K)2}\rangle$ is un-noticeable on the scale of Fig. 4. We therefore conclude that the Raman-induced cross-frequency shift gives the dominant contribution to the total position shift in massive multichannel soliton-based transmission systems at intermediate and large propagation distances.

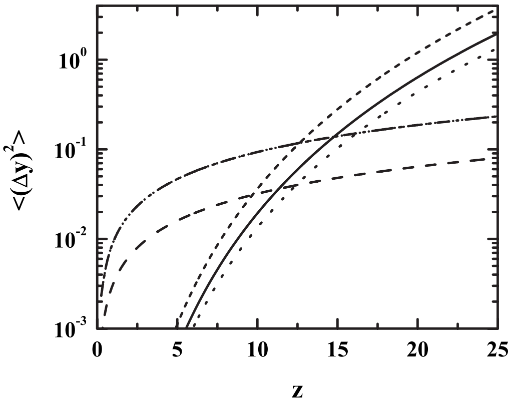

FIG. 4. Second moment of the position shift induced by Raman cross-frequency shift $\langle \Delta y_0^{(c)2}\rangle$ and by Kerr nonlinearity $\langle y_0^{(K)2}\rangle$ vs propagation distance z. The solid, dotted, and short-dashed lines correspond to $\langle \Delta y_0^{(c)2}(z)\rangle$ for the multichannel transmission setups A, B, and C, respectively. The dashed, dashed-dotted, and short-dotted lines represent $\langle y_0^{(K)2}(z)\rangle$ for setups A, B, and C, respectively.

[1] Y. S. Kivshar and B. A. Malomed, Rev. Mod. Phys. **61**, 763 (1989).

[2] U. Frisch, *Turbulence: The Legacy of A. N. Kolmogorov* (Cambridge University Press, Cambridge, England, 1995).

[3] G. P. Agrawal, *Nonlinear Fiber Optics* (Academic, San Diego, 2001).

[4] C. R. Menyuk, Opt. Lett. **20**, 285 (1995).

[5] T. Georges, Opt. Commun. **123**, 617 (1996).

[6] G. E. Falkovich, I. Kolokolov, V. Lebedev, and S. K. Turitsyn, Phys. Rev. E **63**, 025601(R) (2001).

[7] G. Biondini, W. L. Kath, and C. R. Menyuk, IEEE Photon. Technol. Lett. **14**, 310 (2002).

[8] G. Falkovich, I. Kolokolov, V. Lebedev, V. Mezentsev, and S. Turitsyn, Physica D **195**, 1 (2004).

[9] A. Peleg, Phys. Lett. A **360**, 533 (2007).

[10] F. Forghieri, R. W. Tkach, and A. R. Chraplyvy, in *Optical Fiber Telecommunications III*, edited by I. P. Kaminow and T. L. Koch (Academic, San Diego, 1997), Chap. 8, Sec. VIII.

[11] S. Chi and S. Wen, Opt. Lett. **14**, 1216 (1989).

[12] B. A. Malomed, Phys. Rev. A **44**, 1412 (1991).

[13] S. Kumar, Opt. Lett. **23**, 1450 (1998).

[14] Y. Chung and A. Peleg, Nonlinearity **18**, 1555 (2005).

[15] T. I. Lakoba and D. J. Kaup, Opt. Lett. **24**, 808 (1999).

[16] F. Forghieri, R. W. Tkach, and A. R. Chraplyvy, IEEE Photon. Technol. Lett. **7**, 101 (1995).

[17] K.-P. Ho, J. Lightwave Technol. **18**, 915 (2000).

[18] M. Muktoyuk and S. Kumar, IEEE Photon. Technol. Lett. **15**, 1222 (2003).

[19] A. Peleg, Opt. Lett. **29**, 1980 (2004).

[20] A. Peleg and Y. Chung (unpublished).

[21] V. E. Zakharov and A. B. Shabat, Sov. Phys. JETP **34**, 62 (1972).

[22] J. D. Ania-Castañón, Opt. Express **12**, 4372 (2004).

[23] J. D. Ania-Castañón, T. J. Ellingham, R. Ibbotson, X. Chen, L. Zhang, and S. K. Turitsyn, Phys. Rev. Lett. **96**, 023902 (2006).

[24] P. V. Mamyshev and L. F. Mollenauer, Opt. Lett. **21**, 396 (1996).

[25] M. J. Ablowitz, G. Biondini, S. Chakravarty, R. B. Jenkins, and J. R. Sauer, Opt. Lett. **21**, 1646 (1996).

[26] L. F. Mollenauer, A. Grant, X. Liu, X. Wei, C. Xie, and I. Kang, Opt. Lett. **28**, 2043 (2003).

[27] D. F. Grosz, A. Agarwal, S. Banerjee, D. N. Maywar, and A. P. Küng, J. Lightwave Technol. **22**, 423 (2004).

[28] F. M. Mitschke and L. F. Mollenauer, Opt. Lett. **11**, 659 (1986).

[29] J. P. Gordon, Opt. Lett. **11**, 662 (1986).

[30] Y. Kodama and A. Hasegawa, IEEE J. Quantum Electron. **23**, 510 (1987).

[31] R. H. Stolen and W. J. Tomlinson, J. Opt. Soc. Am. B **9**, 565 (1992).

[32] C. Headley III and G. P. Agrawal, J. Opt. Soc. Am. B **13**, 2170 (1996).

[33] F. G. Omenetto, Y. Chung, D. Yarotski, T. Schaefer, I. Gabitov, and A. J. Taylor, Opt. Commun. **208**, 191 (2002).

[34] D. V. Skryabin, F. Luan, J. C. Knight, and P. S. Russell, Science **301**, 1705 (2003).

[35] *Raman Amplifiers for Telecommunications 1: Physical Principles*, edited by M. N. Islam (Springer, New York, 2004).

[36] Raman Amplification, in *Fiber Optical Communication Systems*, edited by C. Headley and G. P. Agrawal (Elsevier, San Diego, 2005).

[37] R. H. Stolen, E. P. Ippen, and A. R. Tynes, Appl. Phys. Lett. **20**, 62 (1972).

[38] P. V. Mamyshev and L. F. Mollenauer, Opt. Lett. **24**, 448 (1999).

[39] C. Xu, C. Xie, and L. Mollenauer, Opt. Lett. **27**, 1303 (2002).

[40] A. R. Chraplyvy, Electron. Lett. **20**, 58 (1984).

[41] D. N. Christodoulides and R. B. Jander, IEEE Photon. Technol. Lett. **8**, 1722 (1996).

[42] The dimensionless z in Eq. (1) is $z=(|\beta_2|X)/(2\tau_0)$, where X is the actual position, τ_0 is the soliton width, and β_2 is the second order dispersion coefficient. The dimensionless retarded time is $t=\tau/\tau_0$, where τ is the retarded time. The spectral width is $\nu_0=1/(\pi^2\tau_0)$ and the frequency difference is $\Delta\nu=(\pi\Delta\beta\nu_0)/2$. $\psi=E/\sqrt{P_0}$, where E is proportional to the electric field and P_0 is the peak power. The dimensionless second order dispersion coefficient is $d=-1=\beta_2/(\gamma P_0\tau_0^2)$, where γ is the Kerr nonlinearity coefficient. The coefficient ϵ_R is given by $\epsilon_R=0.006/\tau_0$, where τ_0 is in picoseconds.

[43] L. F. Mollenauer and P. V. Mamyshev, IEEE J. Quantum Electron. **34**, 2089 (1998).

[44] A. Peleg, M. Chertkov, and I. Gabitov, Phys. Rev. E **68**, 026605 (2003).

[45] A. Peleg, M. Chertkov, and I. Gabitov, J. Opt. Soc. Am. B **21**, 18 (2004).

[46] J. Soneson and A. Peleg, Physica D **195**, 123 (2004).

[47] D. J. Kaup, Phys. Rev. A **42**, 5689 (1990).

[48] A. Hasegawa and Y. Kodama, *Solitons in Optical Communications* (Clarendon, Oxford, 1995).

[49] A. R. Chraplyvy, A. H. Gnauck, R. W. Tkach, J. L. Zyskind, J. W. Sulhoff, A. J. Lucero, Y. Sun, R. M. Jopson, F. Forghieri, R. M. Derosier, C. Wolf, and A. R. McCormick, IEEE Photon. Technol. Lett. **8**, 1264 (1996).

[50] Y. Inada, H. Sugahara, K. Fukuchi, T. Ogata, and Y. Aoki, IEEE Photon. Technol. Lett. **14**, 1366 (2002).

[51] A. Peleg, e-print arXiv:0706.4333.